2019-03-20

Temporal and Spatial Variations of Equatorial Ionization Anomaly Using SWARM Satellite Observation

Tena, Muluken

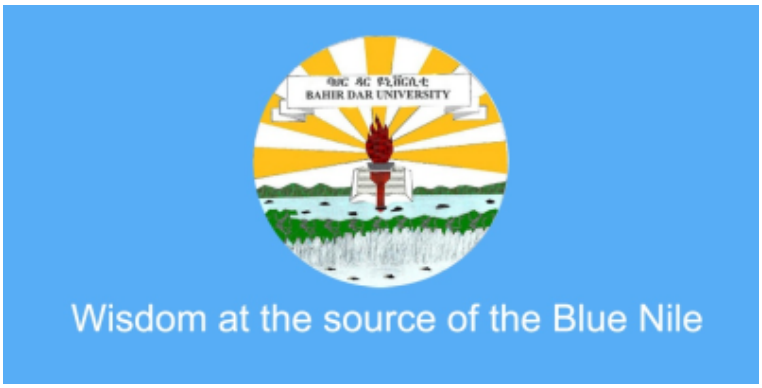

Temporal and Spatial Variations of Equatorial Ionization Anomaly Using SWARM Satellite Observation

Tena Muluken

Bahir Dar

Bahir Dar University

January 16, 2019

CERTIFICATION

The undersigned herby certify that they have read and recommend to the school of postgraduate studies for the acceptance of this project work entitled: "**Temporal and Spatial variation of Equatorial Ionization Anomaly Using SWARM Satellite Observation** by **Tena Muluken** in Partial Fulfillment of the Requirements for the Degree of **MASTER OF SCIENCE IN PHYSICS** at Bahir Dar University..

APPROVED BY:

_____

Melessew Nigussie (PhD), Supervisor

_____

_____

Temporal and Spatial Variations of Equatorial Ionization Anomaly Using SWARM Satellite Observation

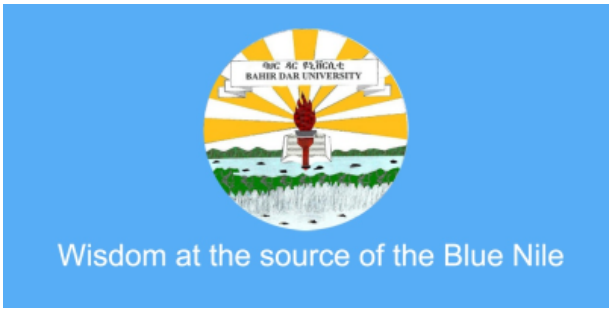

A Thesis Presented to
the School of Postgraduate Studies Bahir Dar University
in Partial Fulfillment of the Requirements for

the Degree of

MASTER OF SCIENCE IN PHYSICS

BY

Tena Muluken
January 16, 2019

AUTHORIZATION TO COPY

Tena Muluken herby authorize the Bahir Dar University to copy and/or release the whole, part of this research work to other researchers and organizations wishing to use the material for reference and/or research purposes.

_____

Acknowledgements

I give all the glory, honour and majesty to the Almighty God who made ways where there seemed to be no way. Thank you Jesus!. I deeply appreciate to my supervisor Dr. Melessew Nigussie for the strong academic supervision, guidance and intelligent suggestions he provided throughout the research period. He has not only been like a father but also a mentor and an inspiration to me. I am equally indebted to my co supervisor Mr. Habtamu Wubie for their constant support in programming and computations without them this dissertation would have been delayed, and for the positive criticism to the timely completion of the research. I am grateful to both of you for investing your time in me. Thank you so much. I would like to thank Head of physics department Dr. Tsegaye Kassa for his emotional support, advice and encouragement. I must express my profound gratitude to all my lecturers who gave me basic foundation in Space Physics. I remain grateful to you all. I am fortunate to have kind and generous colleagues people whose emotional support and enthusiasm have contributed to the success of my work. I thank all of them for their generosity, especially, Dasash Maregu and Biruk Mekuriaw. Finally, I am deeply grateful to my parents for their good moral, and spiritual supports, without which I would not have been able to attain this height. Thank you all.

TABLE OF CONTENTS

List of Figures

Acronyms

ACC - Acclerometer

ASM - Absolute Scalar Magnetometer

CHAMP - Challenging Mini satellite Payload

EFI - Electric Field Instrument

EIA - Equatorial Ionization Anomaly

ESA - European Space Agency

EUV - Extreme Ultra Violet

FORMOSAT-3/COSMIC - Republic of China Satellite-3/Constellation Observing System for Meteorology, Ionosphere and Climate

GPS - Global Position System

IRI - International Reference Ionosphere

LEO - Low Earth Orbit

LP - Langmiur Probe

SROSSC2 - Streched Rohini Satellite Series C2

SWARM - Space Weather Award Receiver Matrix

TII - Thermal Ion Imager

VFM - Vector Field Magnetometer

Abstract

The Earth's ionosphere is part of the upper atmosphere that consists of plasma. Plasma at the equatorial ionosphere is basically produced by photo-ionization of the thin upper atmospheric gases by ultra-violet and shorter wavelength photons from the sun. The EIA is typical plasma dynamic processes of the equatorial ionosphere and characterized as the occurrence of a trough in the ionization concentration at the equator and crests from about $\pm 15^0$ in magnetic latitude in each hemisphere. In this study the ionospheric electron density data is recorded from in situ measurement of SWARM satellite. Specifically, we studied seasonal and longitudinal variations of the EIA for the year of 2014. It is found that the maximum electron density near equatorial anomaly crest yield their maximum values during the equinox months and their minimum values during the June solstice months. During Equinoctial months there is insignificant longitudinal variation in the EIA structure and in June solstice the longitudinal variation of EIA structure is different for different months. The longitudinal variation in the structure of EIA is also significant in those months grouped under December solstice.

CHAPTER 1

Introduction

1.1 Background of the Study

The Earth's ionosphere is the region of electrically conducting plasma ranging from approximately 60 km to over 1000 km. It is formed by different ionization mechanism. For example, EUV radiation and X-rays from the Sun can ionize the neutral atmosphere by striping an electron from the neutral atom that in turn results in the formation of positive ion. Since the neutral atmosphere density at high altitudes is very low, electron and ion produced by the ionization process are free to move around in the plasma, before eventually recombining with ions to form neutral atoms. The ionospheric plasma distribution is highly dependent on both space and time. This plasma distribution variability can be described in terms of the variability on ionospheric quantities such as the electron density, the number of electrons per unit volume, and total electron content, the line integral of electrons along a column of ionosphere per unit area (Schunk and Nagy, 2009).

In the equatorial low-latitude ionosphere at F-region, the ionization density distribution is characterized by a trough at the equator and dual crests on either side of the equator, nearly at about $\pm 15^0$ magnetic latitudes are called as the crests of EIA. Due to the complexity in dynamic pro-

cesses involved in ionization of the equatorial low-latitude ionosphere at F-region, the morphology of this region becomes significant to study (Patel et al., 2017). A large latitudinal disturbance of F region plasma in the lower latitude in the post-sunset hours and the existence of various low-latitude phenomenon observed in the ionospheric total electron content are produced by the growth and decay of EIA (Zhao et al., 2009).

The temporal and spatial variations of EIA's have been studied in different sectors. Yadav et al. (2012) investigated the temporal and spatial variation of the EIA in Indian sector using the multi-station ionosonde data during the 19^{th} (1954-1964) solar cycle. They observed that during solstices, the EIA crest appears earlier in the winter season and the winter crest remains stronger than the summer one during the morning hours. They also demonstrated that during the solar maximum period, the EIA crest in the winter season higher than the other two seasons. However, the transition of stronger anomaly strength from winter to summer season appears during the noon time hours. These observations have been explained by the theory of trans-equatorial neutral wind. Bhuyan and Bhuyan (2008) reported the seasonal variations of the EIA by analyzing the electron density from Indian satellite SROSSC2 at the altitude of 500 km in the 75^0 E longitude sector and IRI2001 model for the years 1995-1999. They found that asymmetric ionization anomaly is prevalent in the equinox and December solstice while the EIA is not so well developed in the June solstice. Lin et al. (2007) investigated the seasonal asymmetry of the north to south EIA crests and their diurnal variations are imaged by using FORMOSAT-3/COSMIC radio occultation observations during July to August 2006. They observed that the stronger electron density of EIA crest appears in the southern (winter) hemisphere while, the northern EIA

crest forms at 12:00 LT and becomes stronger than the southern crest after 15:00 LT. They also showed that the southern/winter EIA crest formed earlier than the northern/summer crest, which is possibly due to summer-winter neutral wind effect. Kassa et al. (2014) investigated the spatio-temporal characteristics of the EIA in the East African sector inferred from ground-based GPS receivers via ionospheric tomography in the period of 2011-2012. They found that the geomagnetic activities have contributed to the daily variations of the EIA. The seasonal reconstructions showed that the magnitude of the peak and the width/thickness of the EIA pronounced during the equinox and weakened during the solstice seasons at 21:00 LT. They also observed that the EIA persisted for longer time in equinox season than the solstice season. The spatial appearance of the northern and southern anomalies are observed starting from 6.12^0 N and 10^0 S respectively along geomagnetic latitudes during equinox season. Tamirat (2008) studied the seasonal, longitudinal, latitudinal and early evening characteristics of the EIA in the Ethiopian sector from the seven years (2000-2006) of CHAMP Satellite's ion density and magnetometer (current profiles) data. They showed that the EIA varies rapidly with latitude as well as with longitude and also exhibits a day to day and seasonal variation. They also observed that the anomaly structure shows stronger symmetry near September and asymmetry near June. The early evening anomaly structures are quite different from the noon times.

1.2 Motivation of the Study

Ionosphere is highly important for long distance communication by reflecting the radio waves back to Earth. Both radio and TV transmissions use radio waves. Since the dynamic changes taking place in the ionosphere affect our communication systems, understanding the physics of this region, therefore, is important to know the changes and design a method to improve our day to day ways of communication.

The focus of this research is in the equatorial sector of the Earth's ionosphere because of the unique phenomena peculiar to this region, namely equatorial ionization anomaly. The geometry of the geomagnetic field lines in the equatorial ionosphere is unique in such a way that the field lines are nearly horizontal. The nearly horizontal geomagnetic field lines combined with the eastward daytime electric field are believed to produce these phenomena. The EIA is an important phenomenon occurring at low-latitudes that results in the highest plasma densities in the ionosphere. Plasma is moved from the region of the magnetic equator to either sides in a range of latitudes of $\pm 15^0$ north and south of the magnetic equator. The general process by which this occurs is known but the understanding of its global behavior is lacking. This is because a detailed observation of this phenomenon over the large scales on which it occurs is difficult (Baumjohann and Treumann, 2004). Because of this reason in this thesis we are interested to characterize equatorial ionization anomaly using very recent SWARM satellite observation.

1.3 Objective

The objective of the study is to characterize the spatial and temporal variations of the equatorial ionosphere using SWARM ion density observation.

1.4 Organization of the Thesis

In this thesis we discussed the introduction part in chapter one. A brief description about the Earth's ionosphere, Equatorial ionization anomaly, Ionospheric dynamo and factor affecting the formation of EIA in chapter two. Ionospheric measuring techniques, Data source and Data analysis presented in chapter three. Results and discussions of the work are presented in chapter four. At the end conclusions are given in chapter Five.

CHAPTER 2

The Earth's Ionosphere

The partially ionized region of the Earth's upper atmosphere, which extends from about 60 km above the surface of the Earth to about 1000 km, is called **ionosphere**. The main source of charged particles of ionosphere is photo-ionization of neutral molecules through EUV and X-rays from the sun. The incident solar radiations of energetic photons interact with neutral atoms and molecules in the upper atmosphere, yielding the outer electrons of such neutral species enough energy to escape the nucleus of the parent atom. Thus an electron becomes free and a positively charged ion is formed, this process is called **photo-ionization**, and by collisions with energetic particles, which is normally known as **impact-ionization**, that penetrate the atmosphere.

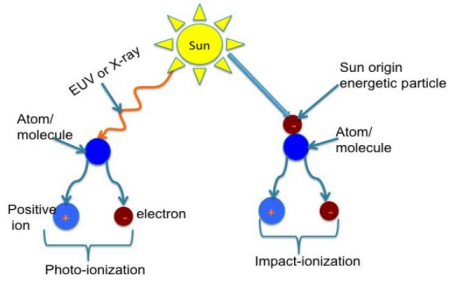

Figure 2.1: Schematics of photo-ionization (left) and impact-ionization (right) (adopted from Nigussie, 2013).

2.1 Layers of the Ionosphere

Based on the electron density profile, the ionosphere is divided into D, E, F regions. The F layer is further divided into F1 and F2 layers during the daytime (Kelly, 1989).

D-region: is the lower part of the ionosphere from altitudes of 70 to 90 km. The major sources of ionization in this region are X-rays, EUV radiation and Lyman- radiation. The ionization rate and the electron density in this region are very low. This layer disappears during nighttime during daytime the D-region can reflect radio waves with reductions to the radio wave signal strength and a major contributor to radio absorption. The electron density of this region varies from $10^8 - 10^9 m^{-3}$.

E-region: is extends to approximately 150 km, this region is mainly formed by soft X-rays and far ultra-violet solar radiation (Kelly, 1989). Normally this layer can only reflect radio waves with frequencies lower than 10 MHz and contribute little absorption for higher frequencies. At night the E-region ionization levels drop because the lack of solar radiation. Daytime electron density of about $10^{11} m^{-3}$ and the nighttime electron density decrease with $5 \times 10^9 m^{-3}$. The most extensively found positive ions in this region are O_2^+ and NO^+ that are produced by the X-rays with wavelength of $1 - 10$ nm and the UV solar radiation in the range $100 - 150$ nm range. In this region strong electric currents are generated by the dynamo effect (Ratcliffe, 1972).

F-region: is the upper ionosphere at altitudes in the range 150 km to 300 km (Kelly, 1989). This region is formed by solar EUV radiation ionizing atomic oxygen. The F layer can be divided into F1 and sub F2 layers. The F1 layer is a daytime phenomenon and forms in the altitude range 140 to 210 km. Most radio waves propagating at oblique incidence that can penetrate the E-region

can also penetrate the F1 layer, so it has little effect on radio communications. with noon peak electron density of $2.5 \times 10^5 cm^{-3}$ and disappears at night when combining with F2 layer to form the nighttime F layer. Ionization of atomic oxygen (O) by He emission lines is probably accompanied by N_2 ionization which disappears after sunset. The F2 layer is the highest layer in the ionosphere and it contain highest free electron density. This region formed at about 300 km with peak electron density values of $10^6 cm^{-3}$ at noon and $10^5 cm^{-3}$ at night times. The height and electron density is highly variable with day, season and sunspot cycle. Ionization is due to EUV radiation ($10 - 100$ nm) of atomic oxygen (O).

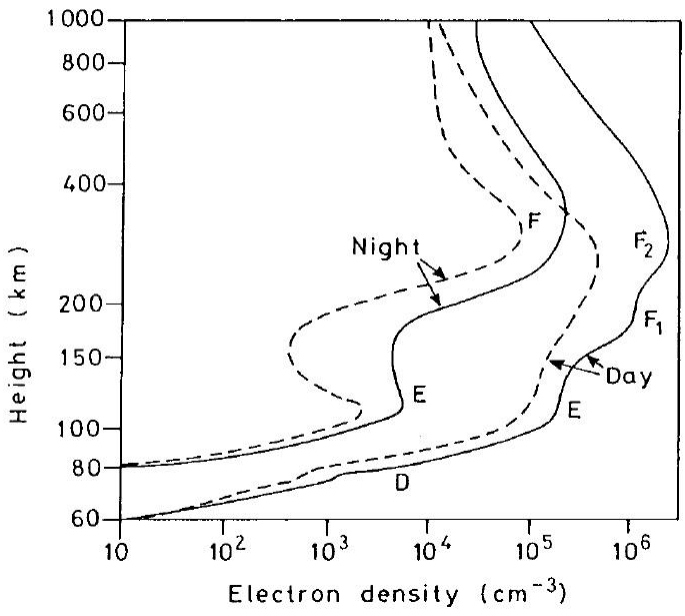

Figure 2.2: Daytime and nighttime vertical electron density profile of ionosphere for periods of solar minimum (dotted curves) and solar maximum (solid curves) (Hargreaves, 1992).

2.2 Geographic Regions of the Ionosphere

In addition to the variation of the electron density with altitude, the ionosphere also shows significant variations with time of day, latitude, longitude and season. A distinctive latitudinal characteristic in the ionosphere is created by the geometry of the Earth's dipolar magnetic field lines. The ionosphere is classified into three latitude regions, low-latitude ($< 20^0$ magnetic latitude), mid-latitude$(20 - 55^0)$, and high-latitude regions $(55 - 90^0)$.

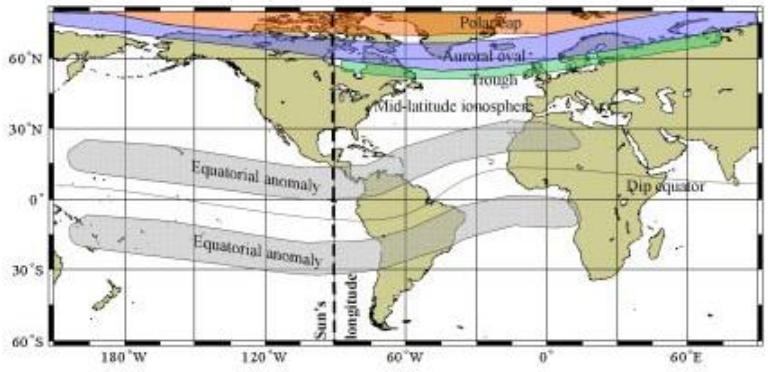

Figure 2.3: Major geographic regions of the ionosphere (Bishop, 1991).

2.2.1 Low-Latitude Ionosphere

At low-latitudes, during the day, one of the most prominent features in the ionosphere is the equatorial anomaly, which is also often called the Appleton anomaly (Appleton, 1946). This feature is distinguished by higher plasma density on both sides of the equator, rather than at the equator itself. The equatorial anomaly is formed as a consequence of $E \times B$ upward plasma drifts associ-

ated with an eastward E field and a northward horizontal B field. The lifted plasma then diffuses downward along the geomagnetic field lines due to the gravitational force and the plasma pressure gradient, and this results in ionization enhancements on both sides of the magnetic equator at $\pm 15^0$ latitudes.

Often, asymmetry is found between the northern and southern anomaly. Due to an inter hemispheric wind blowing from the summer to the winter hemisphere, in the summer hemisphere, plasma moves upward along the geomagnetic field lines, while plasma moves downward in the winter hemisphere. Therefore, the transport of the lifted plasma toward the winter hemisphere is enhanced, and the plasma transport toward the summer hemisphere is decreased. As a result, the equatorial anomaly in the winter hemisphere is generally larger than in the summer hemisphere.

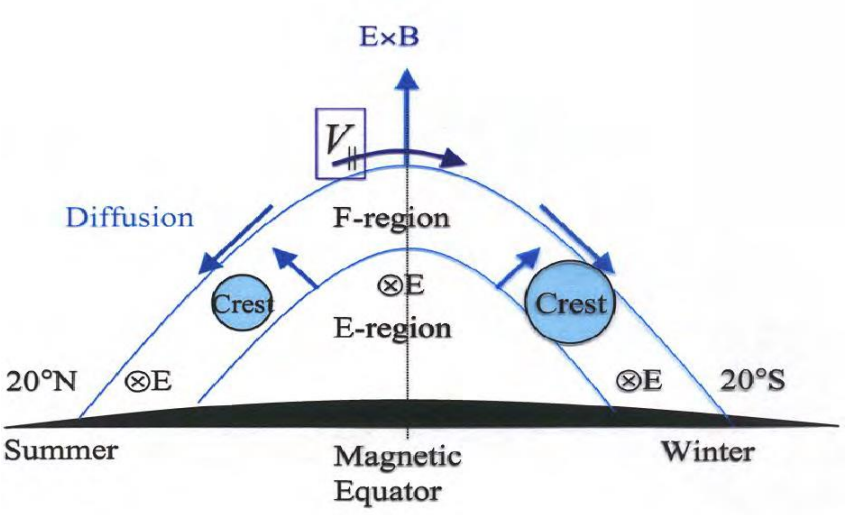

Figure 2.4: Fountain effects and asymmetry of the equatorial anomaly.

2.2.2 Mid-Latitude Ionosphere

This region is a relatively less variable and disturbed region and as a result of this, most of the ionosphere sensing instruments, observations and measurements are best obtained at this region. This latitude is also usually free of the effects imposed by the horizontal magnetic field geometry associated by the equatorial region.

2.2.3 High-Latitude Ionosphere

In the high latitude region collisional ionization is another source of ionization in addition to photo-ionization. This is because geomagnetic field lines are nearly vertical leading to the charged particles descending to E layer altitudes (about 100 km). These particles can collide with the neutral atmospheric gases causing local enhancements in the electron concentration, a phenomena which is associated with auroral activity. Aurora is the most spectacular effect of the physical processes involved and is the visual manifestation of the interaction between the hot magnetospheric plasma and Earth's upper atmosphere (Attila, 1997).

2.3 Ionospheric Variations

The Sun is the main source of ionization energy in the ionosphere. The ionosphere naturally varies with time of day, season and geographic position.

2.3.1 Daily Variations

The day and night electron density of the ionosphere is not the same. Nighttime electron densities are much lower than daytime electron density because in nighttime the recombination rates are higher in the absence of ionization sources. The daytime electron density reaches its peak value at noon hours.

2.3.2 Seasonal Variations

As the Earth revolves around the Sun, a seasonal cycle is generated, determined by which hemisphere the Sun is overhead. It is summer on the hemisphere where the Sun is overhead and winter on the other hemisphere. The Sun is overhead at the equator around the time of the equinoxes. This seasonal cycle causes a corresponding seasonal and spatial variation in the global ionospheric structure. The D, E and F1 region electron densities are greater in summer than in winter. However, the variation in F2 region electron densities is more complicated. In both hemispheres, electron densities generally peak around the equinoxes (Rufus et al., 2012). Around solar minimum the summer noon electron densities are, as expected, generally greater than those in winter, but around solar maximum winter frequencies tend to be higher than those in summer a phenomena called **seasonal anomaly**. In addition, frequencies around the equinoxes (March and September) are higher than those in summer or winter for both solar maximum and minimum (Zhao et al., 2010).

2.3.3 Latitudinal Variations

The daily and seasonal behaviors observed the Sun's position relative to the atmosphere plays significant role in latitudinal variation in the ionospheric electron density because the solar zenith angle (X) measured from the observer's local vertical to the Sun determines the intensity of ionization. This shows that as the solar zenith angle becomes smaller the ionosphere exposes to higher radiation rates and ionization becomes larger.

2.4 Equatorial Ionosphere

The Earth's ionosphere is part of the upper atmosphere that consists of plasma. Plasma at the equatorial ionosphere is basically produced by photo-ionization of the thin upper atmospheric gases by ultra-violet and shorter wavelength photons from the Sun. The dynamics of equatorial ionosphere are greatly depends on plasma transport due to diffusion along geomagnetic field lines, electrodynamics drift and neutral wind effects. At the equatorial regions, the global scale east-west electric fields generated by the action of tidal winds in combination with the north-south geomagnetic field. The common phenomena arising from this region are equatorial electrojet, equatorial ionization anomaly and equatorial spread F (Paul and Dasgupta, 2010).

2.4.1 The Equatorial Ionization Anomaly (EIA)

The plasma behavior can be understood in limited conditions by considering single charged particles and the forces on them (Baumjohann and Treumann, 2004). Consider the motion of a

charged particle with velocity **v** in the presence of external magnetic **B** and electric fields **E**. The force acting on this particle is the sum of electric Coulomb and magnetic Lorentz forces with the resulting motion determined by:

$$m\frac{d\mathbf{v}}{dt} = q\mathbf{E} + q(\mathbf{v} \times \mathbf{B}) \tag{2.1}$$

Where q and m are the charge and mass of the particle respectively. If one is only concerned with the steady state motion of these particles, then the time derivative of the velocity is small and the resulting relation between velocity, electric and magnetic fields is

$$\mathbf{E} = -(\mathbf{v} \times \mathbf{B}) \tag{2.2}$$

Whenever there is a continuous motion of ionospheric plasma in the presence of the Earth's magnetic field, there must exist an electric field perpendicular to both **v** and **B**. Solving for in equation (2.2) gives the expression

$$\mathbf{v} = \frac{\mathbf{E} \times \mathbf{B}}{B^2} \tag{2.3}$$

For the steady state drift of plasma in the presence of electric and magnetic fields. This $\mathbf{E} \times \mathbf{B}$ drifting is independent of charge and both ions and electrons move in the same direction resulting in no net current. Equation (2.3) can be used to gain an understanding the EIA. The equatorial fountain effect, the transport process that moves plasma into the EIA driven by an eastward electric field that exists at low-latitude cause a steady state $\mathbf{E} \times \mathbf{B}$ upward plasma drift. During daytime the eastward dynamo electric field from the E-region maps along the magnetic field to F-region heights above the magnetic equator. The plasma moves upward due to the $\mathbf{E} \times \mathbf{B}$ drift

and then diffuses along the magnetic field to form two crests with maximum ionization density near $\pm 15^0$ geomagnetic latitude and minimum ionization at the geomagnetic equator.

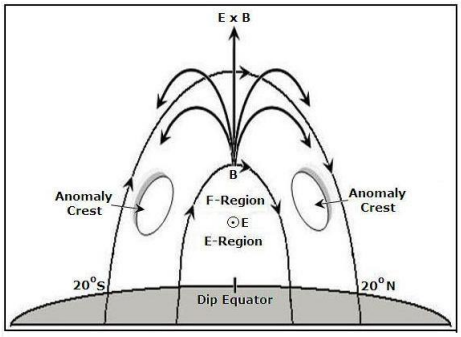

Figure 2.5: Schematic of the formation of the latitude variation of ionization density in the equatorial F-region, known as the equatorial anomaly (Appleton, 1946).

The presence of currents in the ionosphere is interdependent with the local conductivity, which varies with altitude, and the electric fields. The EIA formation requires an understanding of the E and F-region conductivity and how currents are driven by neutral winds. The conductivity of a charged particle in the presence of a magnetic field is given by Ohm's law (Baumjohann and Treumann, 2004).

$$\mathbf{J} = \sigma \cdot \mathbf{E} \tag{2.4}$$

Where $\mathbf{J}$ is the current density and σ is conductivity tensor is given by three components, the Pederson conductivity (σp), which gives currents parallel to $\mathbf{E}$, the Hall conductivity (σH), which gives currents transverse to the applied electric field direction and the Parallel conductivity ($\sigma \parallel$), which gives currents for electric fields aligned with the magnetic field. The complete dependence

of these conductivity upon plasma density, electron-neutral collision frequency, ion-neutral collision frequency and magnetic field strength (Baumjohann and Treumann, 2004). The conductivity parallel to the magnetic field is the largest of the three leading to the conceptual idea of the magnetic field acting as equal potential lines or conductive wires running through the ionosphere. The ionospheric conductivity perpendicular to the magnetic field scale with the collision frequency between the plasma and the neutral atmosphere. At E-region altitudes, where the neutral density and collision frequencies are high, the Pederson conductivity dominates. While in the F-region the Hall conductivity, dominates. The regional motions of the neutral atmosphere, winds or tides, in either the E or F-regions can directly drive currents in the ionosphere by dragging plasma across the magnetic field. Currents are generated because of the different behavior of electrons and ions under the driving force of a neutral wind. The conductivity of the ionosphere then generate internally consistent electric fields for this motion. These fields can then map out of the local region where they are generated along the highly conductive magnetic fields.

2.5 Ionospheric dynamo

Low-latitude electric fields, plasma drifts and ionospheric currents result largely from the dynamo action of E and F neutral winds (Richmond, 1994). The E layer dynamo electric field mapped along the highly conducting magnetic field lines controls the plasma dynamic/transport of the equatorial F-region during the day, whereas the F layer dynamo electric field can develop only during the night as result of the disappearance of E layer conductivity after sunset.

2.5.1 E-Region Dynamo

The electric fields are generated in the E-region by ionospheric dynamo driven by atmospheric tidal winds (Heelis, 1974). The winds, which are established by the absorption of solar radiation in the stratosphere and troposphere, affect the movement of charged particles. Ions and electrons assumes a cyclotron movement in the present of $\mathbf{B}$. The interaction between the tidal wind ($\mathbf{U}$) and $\mathbf{B}$ gives rise to a relative movement between the ions and electrons which leads to an induced electric field as a result of $\mathbf{U} \times \mathbf{B}$. The induced current associated with this is not stationary, i.e. $\nabla \cdot J \neq 0$. This makes electric field polarization ($\mathbf{E_p}$) to be established in the E-region with out any current divergent. The total electric field in this ionospheric region:

$$\mathbf{E} = \mathbf{E_p} + (\mathbf{U} \times \mathbf{B}) \tag{2.5}$$

Substituting equation (2.5) in (2.4) we have the current flowing in a conductor in this region is not divergent

$$\mathbf{J} = \sigma(\mathbf{E_p} + (\mathbf{U} \times \mathbf{B})) \tag{2.6}$$

By considering the dynamo region as a conductive thin plate subjected to a constant zonal electric field ($\mathbf{E_X}$), perpendicular to $\mathbf{B}$ (Kelly, 2009). The $\mathbf{B}$ and the $\mathbf{E}$ in the region are perpendicular to each other. There are essentially two types of current in the equatorial E-region, which are the Hall and Pederson current. The Hall current ($\sigma_H \mathbf{E_X}$) flows in the direction perpendicular to both electric field ($\mathbf{E}$) and the $\mathbf{B}$, while the Pederson current ($\sigma_P \mathbf{E_Z}$) flows parallel to the electric field ($\mathbf{E}$) and perpendicular to $\mathbf{B}$. The Hall current cannot flow across the boundary and this leads to accumulation of charges at both boundary. These accumulated charges gives rise

to upward electric field polarization. In response to this polarization, the Hall current ($\sigma_H \mathbf{E_X}$) and the Pederson current ($\sigma_P \mathbf{E_Z}$) are in steady state but no vertical current can flow hence both Pederson and Hall current cancels. This gives $\sigma_H \mathbf{E_X}$=$\sigma_P \mathbf{E_Z}$ dividing both side by σ_P

$$\mathbf{E_Z} = (\frac{\sigma_H}{\sigma_P})\mathbf{E_X} \tag{2.7}$$

In the horizontal direction the current add up and then form an intensified field called **equatorial electrojet**:

$$\mathbf{J_X} = \sigma_H \mathbf{E_Z} + \sigma_P \mathbf{E_X} \tag{2.8}$$

Substituting equation (2.7) in (2.8) we have:

$$\mathbf{J_X} = [\frac{\sigma_H^2}{\sigma_P^2} + 1]\sigma_P \mathbf{E_X} = \sigma_C \mathbf{E_X} \tag{2.9}$$

Where σ_C= $[\frac{\sigma_H^2}{\sigma_P^2} + 1]\sigma_P$ is called Cowling conductivity. The equatorial electrojet is determined by tidal winds that create the global component of the daily zonal electric field measured at the equator. It is the strong current around $\pm 3^0$ latitude of the geomagnetic equator.

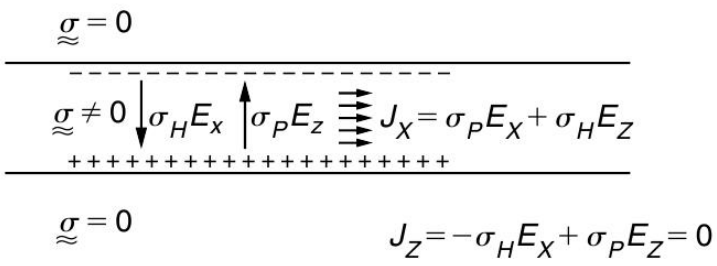

Figure 2.6: E-region electrodynamics (Kelly, 2009).

2.5.2 F-Region Dynamo

The E-region plasma density and neutral winds are controlled the E-region dynamo. The electric fields generated in this way dominate in the day but subside at night. After sunset the ions in E-region quickly recombine and the E-region dynamo process stops. At this point the F-region dynamo, where recombination happens much slower, becomes important. Zonal neutral winds or east/west winds in the F-region create a meridional current system and in the process generate a vertical polarization electric field (Sojka and Schunk, 1985). During the day this polarization field is weak as the E-regions are highly conductive across the field lines and this meridional current loop can close in the E-region. However, during the night, the E-region conductivity drops, and the vertical electric field grows in the F-region which creates an $\mathbf{E} \times \mathbf{B}$ plasma drift. Therefore, F layer dynamo plays a dominant role in the night time EIA development (Rishbet, 1971; , 1972).

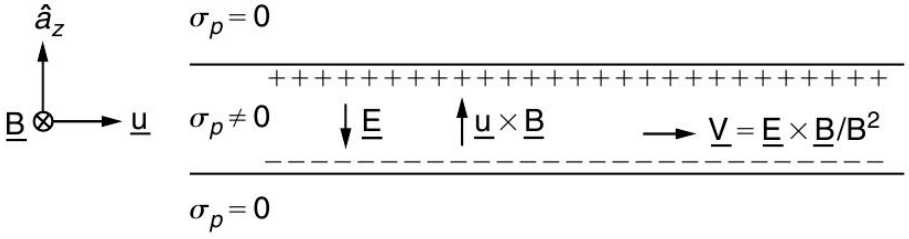

Figure 2.7: F-region electrodynamics (Kelly, 2009).

2.6 Factors Affecting the EIA

The EIA development depends on a complex coupling of a number of atmospheric processes and winds in the upper atmosphere. Two different processes, the E and F-region dynamos control the EIA formation during the day and its evolution during the night. The EIA shows considerable variability with local time, longitude and season. A description of a few factors creating variability in the EIA.

2.6.1 Magnetic Equator

The direction of the Earth's magnetic field can be given in terms of magnetic inclination and declination. The magnetic or the dip equator are the latitudes where the inclination or dip is zero. The magnetic equator does not follow the geographic equator. Its alignment from the geographic equator varies considerably with longitude but neutral atmospheric winds are generally aligned with the geographic equator. At longitudes where the magnetic equator lies far off from the geographic equator, an asymmetry in the equatorial arcs is expected due to variations of the neutral winds with latitude. The Sun is aligned with the magnetic equator and the neutral winds are assumed to blow symmetrically on to both sides of the dip equator. As the Earth rotates, the magnetic dipole shifts with respect to the Sun and the sub solar point lies entirely to the north of the dip equator even during equinox conditions (Sojka and Schunk, 1985). This resulting asymmetry partially explains the longitudinal variability in the structure of the equatorial arcs.

2.6.2 F-Region Neutral Winds

The north and south peaks of the EIA have asymmetries during summer or winter solstice due to the nature of the resulting meridional neutral winds in the F-region. The winds blow away from the sub solar point which is generally located north or south of the EIA. During solstice, winds from the sub solar point tend to push the plasma into the winter hemisphere and the anomaly is more developed on to one side of the magnetic equator. Thus, a seasonal shift in the sub solar point accounts for some of the asymmetric seasonal variability in the EIA. This same process is responsible for a shifting of the latitude at which the peak density in the EIA occurs. At a certain altitude the diffusion of the plasma down and along flux tubes in the equatorial fountain can be balanced against the neutral north or south winds, the plasma tends to lie suspended if the wind is against the downward drift. This piling of plasma will eventually be where we see the peaks of the EIA occur thus moving the arc closer to the geomagnetic equator.

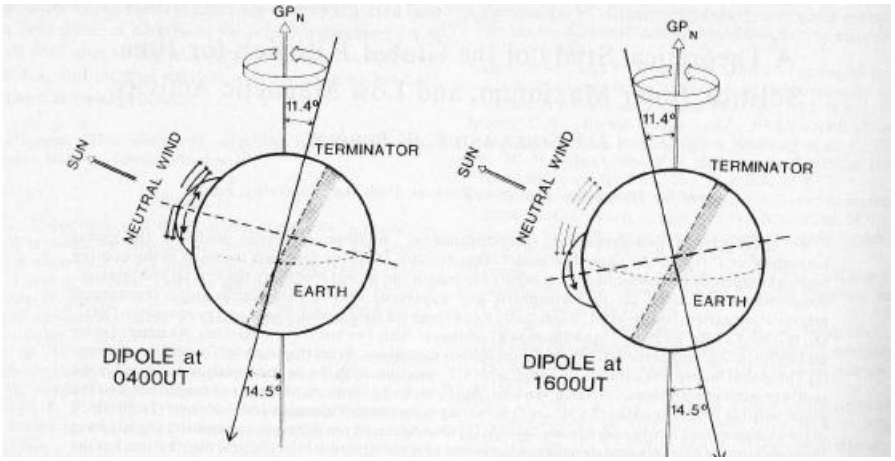

Figure 2.8: F-region meridional winds (Shankar, 2007).

CHAPTER 3

Ionospheric Measuring Techniques

The Langmuir probe (LP) is part of the Electric Field Instruments (EFI) used to measure electron and ion densities as well as the temperatures in plasma's, with SWARM satellite for low-latitude Low Earth orbit (LEO) missions. LP technique for in situ measurement of plasma parameters has been around for eight decades. The temperature and density of the plasma in the equatorial ionosphere are important parameters for understanding the general characteristics of the ionosphere. The probe electron density of the plasma is given by

$$n_e(x) = n_o exp(\frac{e\phi(x)}{K_B T_e}) \tag{3.1}$$

Where, $\phi(x)$ is the potential at an arbitrary point in the plasma, K_B is Boltzmann constant, n_e is the electron density, n_o is the undisturbed plasma density, and T_e is the electron temperature.

This thesis mainly uses in situ measurement using SWARM satellite observation data. In situ measurements of plasma density in the F-region of ionosphere provides useful information about the location of the EIA, its spatial and temporal extent.

The SWARM Satellite

SWARM is a European Space Agency (ESA) mission to study the dynamics of the Earth's magnetic field and its interactions with the Earth system (Friis-Christensen et al., 2008). SWARM consist of three identical satellites namely Alpha (SWARM A), Bravo (SWARM B) and Charlie (SWARM C). The three satellites were launched together on November 2013. The constellation are almost circular, near-polar orbiting spacecraft enables a homogeneous and almost complete global coverage of the Earth. They are not Sun synchronous orbits and they allow the satellites to move rapidly through local time. The payload of the three spacecraft consists of the following instruments:

1. Vector Field Magnetometer (VFM): Linear and low-noise measurements of the Earth's magnetic field vector components.

2. Absolute Scalar Magnetometer (ASM): Calibration of the main instrument VFM.

3. Electric Field Instrument (EFI): Measurement of ion density, drift velocity and electric field.

4. Accelerometer (ACC): Measurement of non gravitational accelerations like air drag, winds and solar radiation pressure.

3.1 Data Source and Data Analysis

3.1.1 Data Source

The data which has been used for this thesis is retrieved from an Low Earth Orbiting (LEO) SWARM satellite data which consists of three identical satellites A, B and C. Two satellites, SWARM A and C, are flying side by side in orbits separated by only 1.4^0 in longitude and at an altitude of about 460 km with an inclination of 87.4^0. The third spacecraft SWARM B, orbits the Earth at about 530 km with an inclination 88^0. The plasma density observations from SWARM C are almost identical with those from SWARM A. Therefore, we mainly used the data from an observation of SWARM A constellation. In the current study, our analysis depends on only data recorded by Electric Field Instrument data $(EFIA)$ at SWARM A. The $EFIA - LP - 1B$ product contains plasma data from the Electric Field Instrument (EFI) which consists of the LP and the Thermal Ion Imager (TII). The plasma product from the $EFIA - LP - 1B$ file contains two important plasma parameters: the electron density and the electron temperature in exact geographic satellite position, our analysis used only the electron density product data.

3.1.2 Data Analysis

Since the inclination of the orbit of the satellite is very high, the path followed by the satellite has a polar orbit characteristics as shown in figure 3.1. That means as the satellite takes a single pass from one pole to the other it covers all latitudinal values where as its longitude is almost constant.

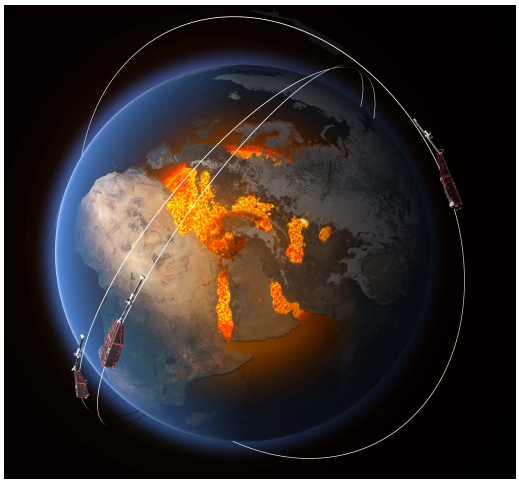

Figure 3.1: Orbital dynamics of the satellite.

Figure 3.2 demonstrates the temporal variations of the geographic latitude position of the satellite traced by the satellite in a single day (January 1, 2014). Since the longitude of the satellite varies rapidly in the polar region, we didn't consider its motion for latitudes greater than 60^0 and less than -60^0. Each single pass from one pole to the other is indicated by numbers as shown in figure 3.2.

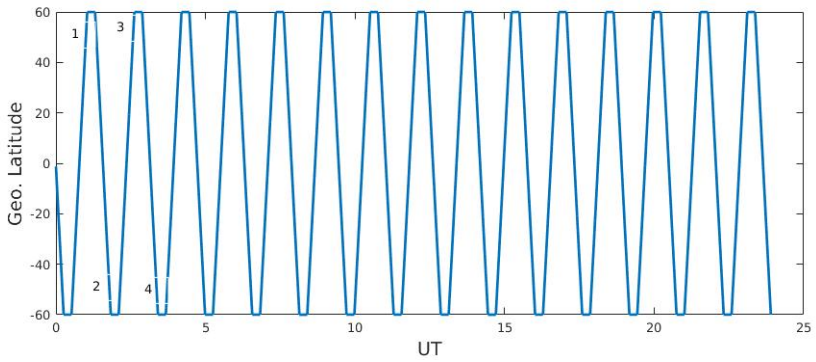

Figure 3.2: Temporal variation of latitudinal position of SWARM A for January 1, 2014.

In order to exactly access individual passes separately we have developed an algorithm and write a corresponding MATLAB codes for the algorithm. Figure 3.3 indicates that the longitudinal positions of the satellite in a single pass is almost constant.

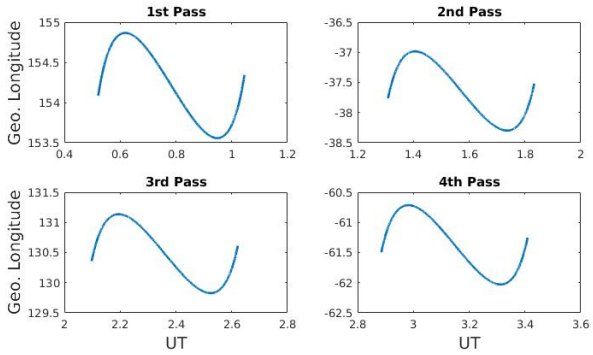

Figure 3.3: Variation of longitude with time for January 1 from selected pass.

In order to obtain a single longitudinal value for each pass, we calculated the mean of the longitudinal values traced by the satellite in a given pass.

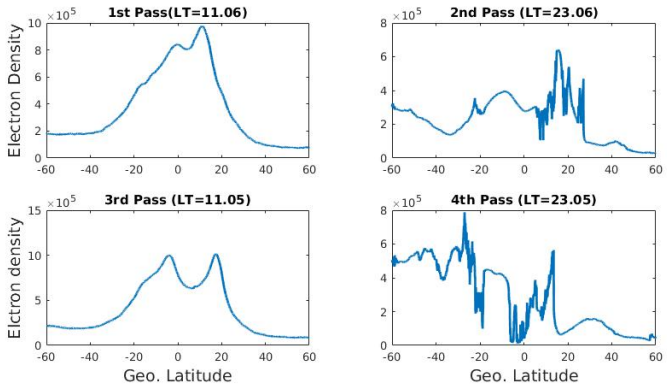

Figure 3.4: Variation of electron density with latitude for January 1 from selected pass.

This enables as to determine the distribution of electron density at a single longitude but at different latitudinal values for each pass. The irregular distribution of electron density observed in the two graphs is due to the night time occurrence of ionospheric irregularities. The local time for each pass is calculated from the corresponding mean longitudinal values of the pass by combining the electron density distribution with latitude for all passes as show in figure 3.4. We produces the following contour map of electron density and line on the map shows the position of dip equator.

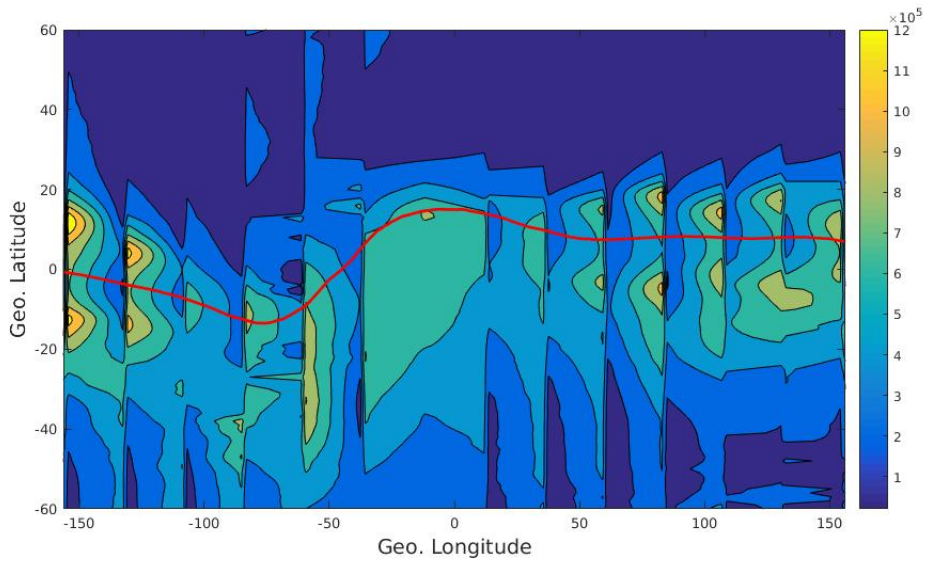

Figure 3.5: Variation of electron density with geographic latitude and longitude for January 1, 20014.

CHAPTER 4

Results and Discussions

In this study we have characterized EIA for the year 2014, using SWARM satellite observation. Manly we have analyzed longitude and seasonal variations of EIA using the data obtained from SWARM satellite observation.

Ionization in the F-region is directly proportional to the strength (intensity) of the solar ionizing radiation. On the other hand, the intensity of solar radiation is highly dependent on the position of the Earth relative to the Sun. Since the relative position of Earth with respect to Sun varies with season, the intensity of the ionizing radiation also varies significantly with season. This significant variation of intensity of the solar radiation leads to another important and significant seasonal variation of electron density.

In this thesis we will follow Koh and Shigeto (2004) approach's to classify the whole months of the year in to three seasons. Koh and Shigeto (2004) have grouped (September, October, March, April and February) in to season of equinox, where as (May, June, July and August) are grouped in to seasons of summer in the northern hemisphere (June solstice), finally (November, December and January) are grouped as season of summer in the southern hemisphere (December solstice). The latitudinal and longitudinal variations of ionospheric electron density for all months in the year of 2014 are depicted using contour plots. The red color in all contour plots represents

the peak electron density. As contour plots clearly indicates for all months the electron density exhibit large structure with a trough near the magnetic equator and crests both sides of the dip equator. A depression in ionization density at the dip equator and an exhibition of two peaks on either sides of the geomagnetic equator is called EIA. All contour polts indicate that, the position and strength of the EIA is easily distinguishable for all months in the given year. According to Mitra (1946), the trough exists because plasma produced by photo-ionization at heights over the magnetic equator diffuses downwards and outwards to the north and south leaving depletion at the equator.

4.1 Seasonal and Longitudinal Variation of EIA

Contour plots in figures 4.1 to 4.3 indicate that seasonal and longitudinal variation of EIA for equinoctial months. During equinoctial months negligible trans-equatorial component of the neutral wind and vertical $E \times B$ plasma drift will cause symmetric development of EIA crest in both sides of the geomagnetic equator. The maximum electron density is observed in those months this is because during equinoctial months the sun shines its radiation around the equator and the temperature at the equator is hotter than at the other latitudes. However, in the case of imbalanced meridional components of neutral wind on both sides of magnetic equator, induced field aligned motion of ions can cause some equinoctial asymmetric development of EIA crest along the magnetic equator (Bailey et al., 2000). Figure 4.1 in the month of September; indicate that the strength of the EIA crest in the northern hemisphere is higher than that of the southern

hemisphere. This may be due to meridional wind blowing from southern hemisphere to the northern hemisphere in this case high electron concentration is exhibit in the northern hemisphere than the southern hemisphere this should be result for strong EIA crest value is exist in the northern hemisphere.

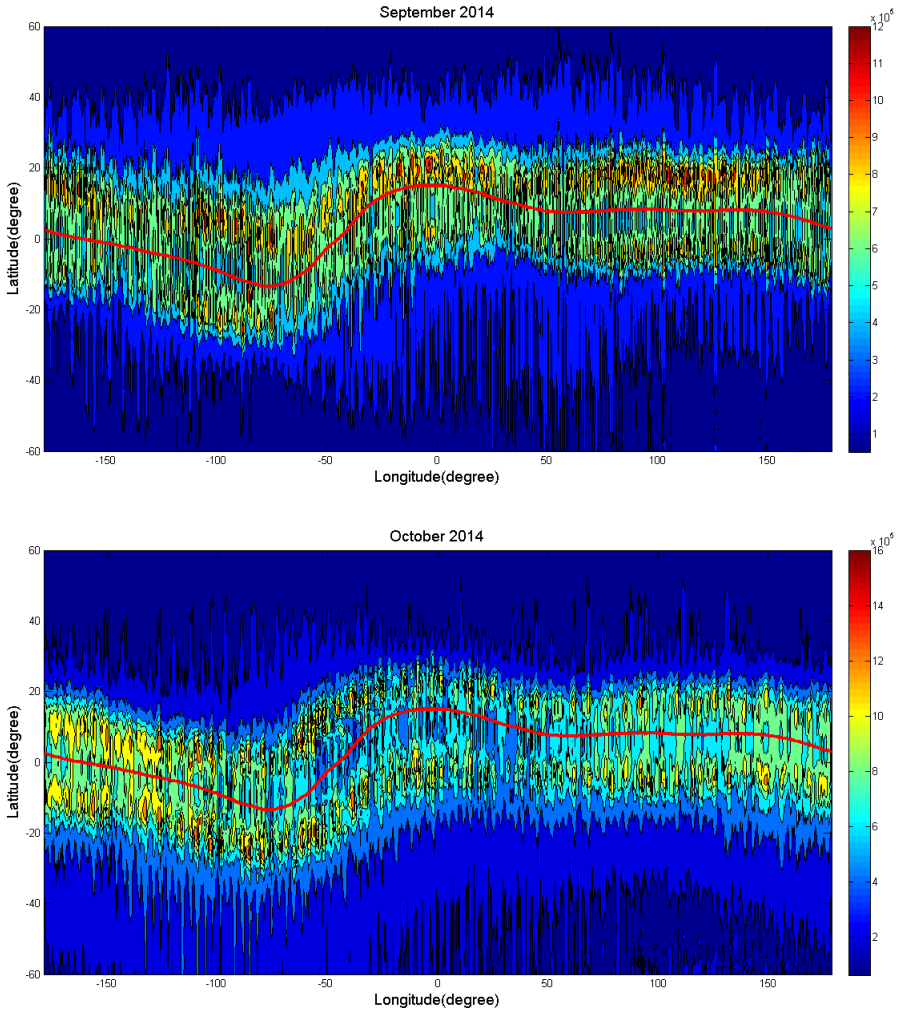

Figure 4.1: Variation of EIA for equinoctial month's.

The longitudinal variation in the structure of EIA is found to be common and prominent. The EIA

longitudinal structure is vary from season to season. Figures 4.1 to 4.3 show that during equinoctial months, there is insignificant longitudinal variation in the structure of EIA for all longitudinal sectors. This may be due to the fact that during equinoctial months the incident angle of solar EUV illumination over the geomagnetic equator is similar at most at all longitudinal sectors.

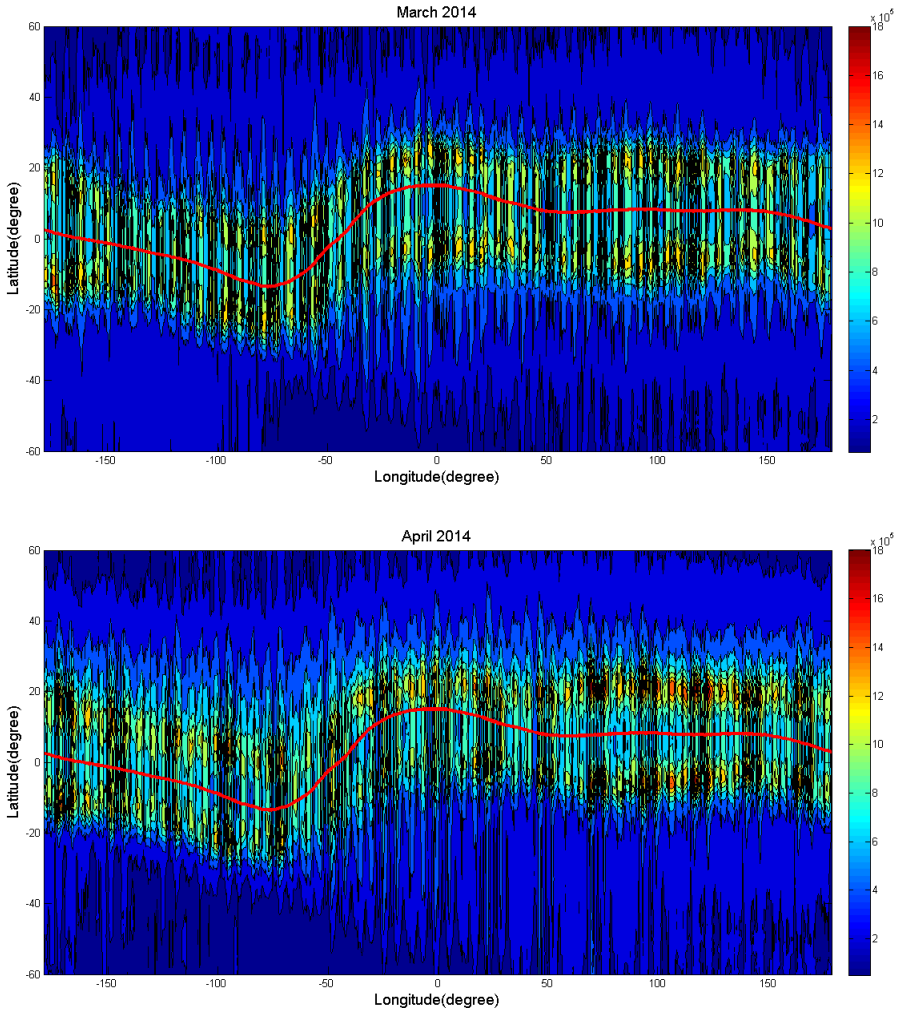

Figure 4.2: Variation of EIA for equinoctial month's.

During equinoctial months there is no significant differences in the north south asymmetry of the

EIA crest, which seems to indicate that the longitude variation of the east west electric field and neutral winds are small effect on at all longitudinal regions during these months.

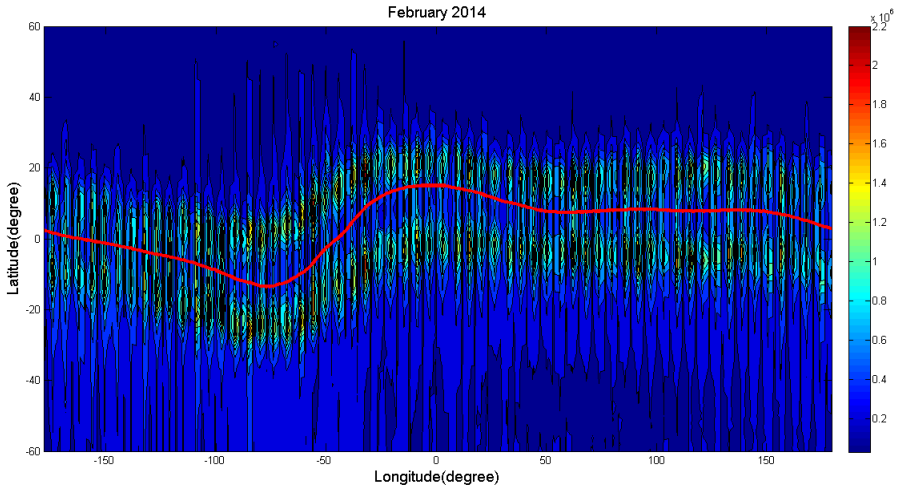

Figure 4.3: Variation of EIA for equinoctial month.

Figures 4.4 to 4.8 clearly indicate that the EIA crest values in the summer hemisphere are relatively greater than those in the winter hemisphere. This mainly because of the fact that in the winter hemisphere the photo-ionization at the equator decrease because the sun overhead moves to summer hemisphere and fountain effect is expected to be weak and the wind pushes the plasma from winter hemisphere to the summer hemisphere. This gives rise to more ionization and large EIA crest values in the summer hemisphere than in the winter hemisphere. On the other hand, the summer anomaly characterized by higher electron density in the summer hemisphere than in the winter hemisphere.

During solstice seasons is associated to trans-equatorial neutral winds and equatorial fountain effect processes as discussed below:

1. In the winter hemisphere, the electrodynamics transport of plasma due to equatorial fountain process will be in the same direction to the transport due to trans-equatorial neutral wind. Therefore, the combined action of equatorial fountain and trans-equatorial wind pushes the plasma down ward along the field line in to the region of higher recombination rate in the winter hemisphere causing weakening of winter EIA crest (Sai and Tulasi, 2017).

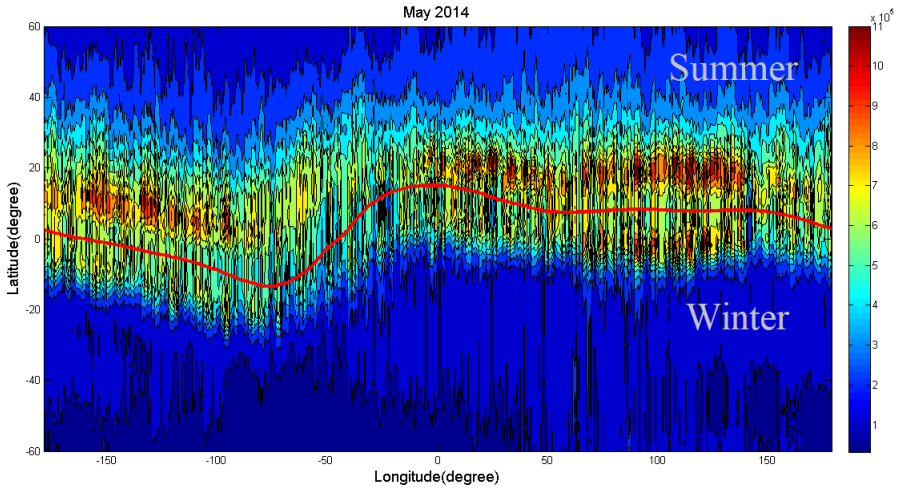

Figure 4.4: Variation of EIA for June solstice month.

2. On the other hand, the transport due to equatorial fountain process is in opposite direction to field aligned upward transport due to neutral wind in the summer hemisphere. As a result, the plasma accumulates at relatively higher altitudes when rate of recombination is low and stronger EIA crest forms in the summer hemisphere (Sai and Tulasi, 2017).

Another interesting feature that can be observed from figures 4.4 to 4.8, the EIA crest values are in general significantly higher during December solstice than June solstice (Sai and Tulasi, 2017). Generally, filed aligned plasma transport produced by neutral wind is known to alter EIA structure, especially during solstice seasons.

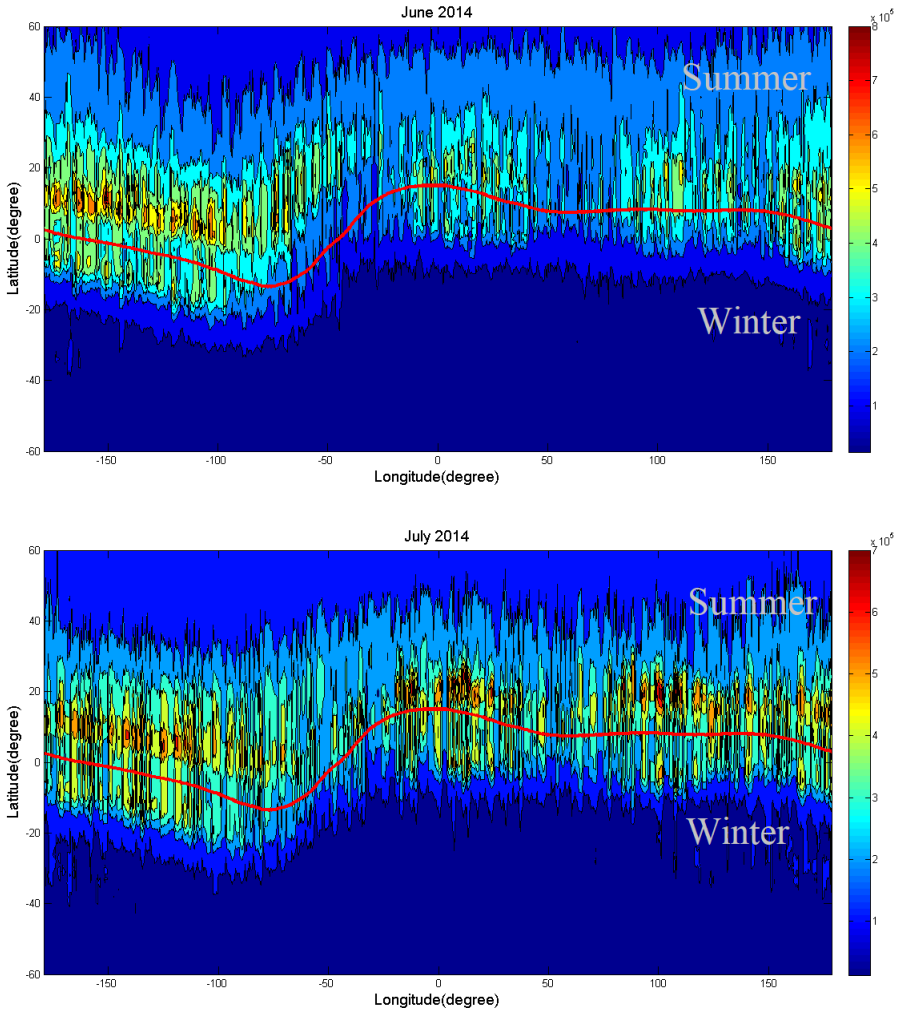

Figure 4.5: Variation of EIA for June solstice month's.

During season of June solstice (northern summer) the longitudinal variation of EIA structure

is different for different months. As clearly shown in the contour plot, in the month of May from figure 4.4, the EIA crest value is almost uniform at all longitudinal sectors in the northern hemisphere. But in the reverse way, the EIA crest values in the southern hemisphere varies significantly as we go from western longitudinal regions to eastern longitudinal regions. Significant variation in the structure of EIA is also observed during June as shown in figure 4.5. The EIA crest values are very large in the western longitudinal sector as compared to other longitudinal sectors. From this month the EIA crest value of the northern hemisphere in the western region is greater than that of the eastern region. Similar longitudinal variation is also observed in July and

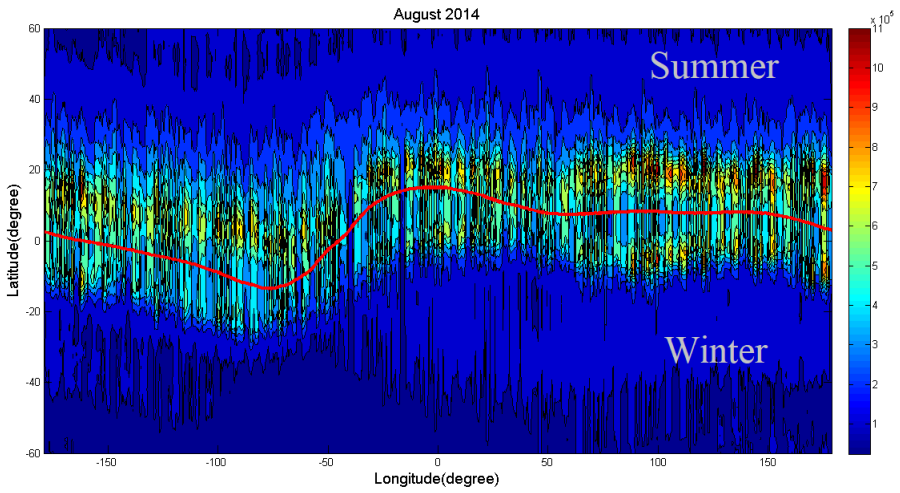

Figure 4.6: Variation of EIA for June solstice month.

August. In the month of July from figure 4.5, the EIA crest values of the northern hemisphere in the western longitudinal sector shows insignificant variation than in the eastern longitudinal sector, that means strong variation in EIA crest is observed in the eastern region than in the western region. For the month of August from figure 4.6, the EIA crest values of the northern and

southern hemisphere in the eastern region is greater than that of the western region. insignificant longitudinal variation in EIA structure is observed during August than during other months in June solstice.

The longitudinal variations in the two solstices may be caused by the longitudinal variation of geomagnetic declination and westward winds. Generally, in June solstice months the structure of EIA crest is stronger in the northern hemisphere for all longitudinal sectors. We assumed that the field aligned component of daytime west ward zonal winds enhances the field aligned component of the summer to winter (north to south) meridional winds in the longitude range with positive declination (eastward) and opposes the field aligned component in the longitude range with negative declination (westward). Therefore the structure of EIA crest value is varies with magnetic declination (Huang et al., 2010).

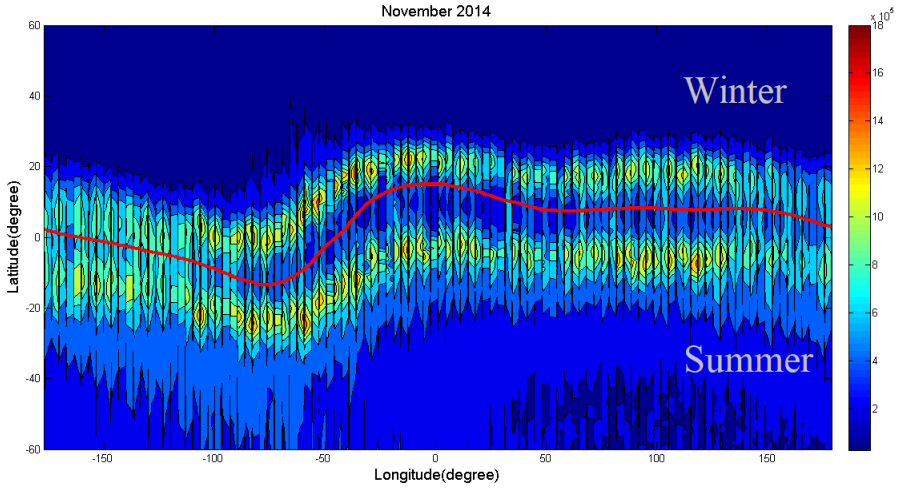

Figure 4.7: Variation of EIA for December solstice month.

The longitudinal variation in the structure of EIA is also significant in those months grouped under December solstice. During November as shown in figure 4.7, the EIA crest values in the northern and southern hemispheres show significant variation in all longitudinal regions.

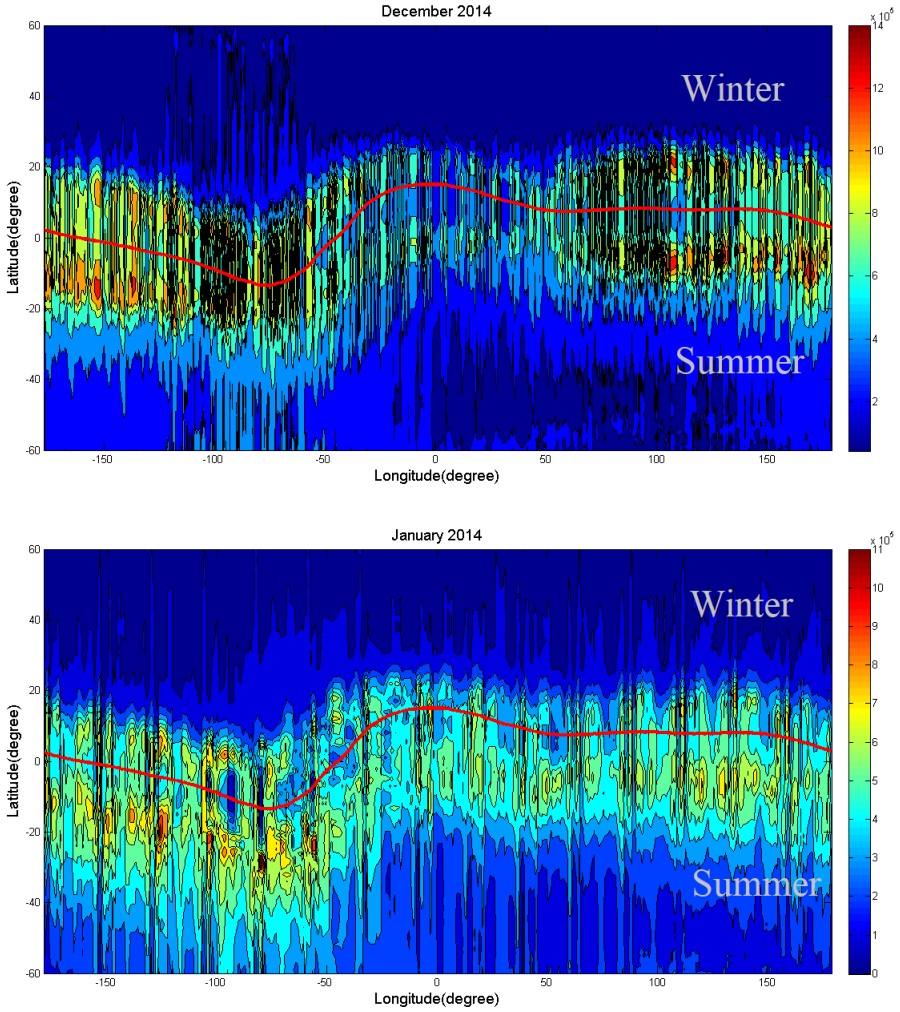

Figure 4.8: Variation of EIA for December solstice month's.

Comparatively strong EIA structure is observed in the western region of the globe than in the eastern region of the globe. Very significant variation of EIA development is observed in the

month of December. As can be seen from figure 4.8 for the month of December, the EIA crest values in both northern and southern hemisphere is very large in both eastern and western longitudinal sectors. As seen from the contour plot of January in figure 4.8, the EIA crest values in the western region are relatively stronger than those in the eastern region in both hemisphere. And in the southern hemisphere, significant longitudinal variations of the ionospheric electron density or EIA crest is observed. The significant longitudinal variation of the declination angle affects very differently the plasma transport along the field line via interaction between the plasma and zonal neutral wind. The change in the magnetic and electric fields with longitude results in the variation of the vertical drift velocity of plasma over the equator. Since vertical drift velocity is the major cause for the development of EIA. Its longitudinal variation cause different structure of EIA development at different longitudes. For example, The total magnetic field intensity at the equator has minimum value near 300^0 and maximum near 100^0. This result corresponds to greater vertical plasma drift velocity near 300^0 than near 100^0 via the known formula of $\mathbf{v} = \frac{\mathbf{E}\times\mathbf{B}}{B^2}$ (Sagawa et al., 2005). (Scherliess and Fejer, 2008) showed that the upward plasma drift velocity over the equator, which corresponds to zonal electric field strength exhibits both longitudinal and seasonal dependencies.

CHAPTER 5

Conclusions

We have characterized the phenomenon in the EIA region from the in situ electron density measurements of SWARM A satellite in the year of 2014. We examine the dependence of the EIA on longitude and seasons. The major findings of this study are as follow:

The seasonal distribution of the events shows that the summer events are located further from the magnetic equator in the northern hemisphere and shift their locations into the southern hemisphere in the December solstice months especially in January, while equinox events are centered along the magnetic equator.

In general, electron concentrations in the ionosphere are controlled by EUV radiation (photo-ionization). Photo-ionization caused by solar EUV radiation can play a role in the production of the EIA crest.

Finally we conclude that the seasonal variation of EIA is maximum on the equinox months especially on February, April and March and minimum peak value of EIA has recorded on the June solstice months which is during July and also December solstice months during January.

The longitudinal variation in the EIA structure is insignificant in equinoctial months, different longitudinal EIA structure for different months are exhibit in June solstice and significant longitudinal EIA structure is recorded in December solstice months.

References

Appleton, E. Two anomalies in the ionosphere. *Nature*, **157**, 1946.

Attila, K. Global ionospheric total electron content mapping using the global positioning system. *University of New Brunswick, Canada*, 1997.

Baumjohann, W. and Treumann, R. Basic Space Plasma Physics. *Imperial College Press*, 2004.

Bailey, G., Su, Y., and Oyama, K. Yearly variations in the low-latitude topside ionosphere. *Ann. Geo phys*., **18**, 2000.

Bhuyan, P. and Bhuyan, K. The equatorial ionization anomaly at the topside F region of the ionosphere. *Adv. Space Res*., **43**, 2008.

Friis-Christensen, E., Luhr, H., Knudsen, D., and Haagmans, R. Swarm an earth observation mission investigating Geo space. *Adv. Space Res*., **41**, 2008.

Heelis, R. Electrical coupling of the E and F-regions and its effects on F-region drifts and winds. *Space Sci*., **22**, 1974.

Huang, C., Rich, F. and Heelis, R. Longitudinal and seasonal variations of the equatorial ionospheric ion density and eastward drift velocity in the dusk sector. *J. Geophys. Res*., **115**, 2010.

Kassa, T., Damtie, B., Bires, A., Yizengaw, E. and Cilliers, P. Spatio-temporal characteristics of

the Equatorial Ionization Anomaly (EIA) in the East African region via ionospheric tomography during the year 2012. *Adv. Space Res*., **55**, 2015.

Kelly, M. The Earth's Ionosphere: Plasma Physics and Electrodynamics. *Academic Press*., 1989.

Kelley, M. The Earth's Ionosphere: Plasma Physics and Electrodynamics, 2nd ed. *Academic Press*, 2009.

Koh, I. and Shigeto, W. Effects of zonal and meridional neutral winds on the electron density and temperature at the height of 600 Km. *Japan Aerospace Exploration Agency*, **18**, 2004.

Lin, C., Liu, J., Fang, T., Chang, P. and Tsai, H. Motions of the equatorial ionization anomaly crests imaged by FORMOSAT-3/COSMIC. *Geo phys. Res*., **34**, 2007.

Mitra, S. Geomagnetic control of region F 2 of the ionosphere. *Nature*, **158**, 1946.

Patel, N., Karia, S. and Pathak, K. GPS-TEC variation during low to high solar activity period (2010-2014) under the northern crest of Indian equatorial ionization anomaly. **8**, 2017.

Paul, A. and Dasgupta, A. Characteristics of the equatorial ionization anomaly in relation to the day to day variability of ionospheric irregularities around the post sunset period. *Radio Sci*., **45**, 2010.

Ratcliffe, J. An introduction to the ionosphere and magnetosphere. *Cambridge University Press*, 1972.

Richmond, A. The ionospheric wind dynamo effects of its coupling with different atmospheric regions. *American Geophysical Union*, 1994.

Rishbet, H. Polarization fields produced by winds in the equatorial F-region. *J. Atmos. Terr.phys*., **34**, 1971, 1972.

Rufus, S., Rabiu B., Olakunle O. and Keith, G. Variation of total electron content (TEC) and their effect on GNSS over Akure. *Nigeria*, 2012.

Sagawa, E., Immel, T., Frey, H. and Mende, S. Longitudinal structure of the equatorial anomaly in the night time ionosphere observed by IMAGE/FUV. *J. Geo phys. Res*., **110**, 2005.

Sai, G. and Tulasi, R. Ionospheric winter anomaly and annual anomaly observed from FORMOSAT-3/COSMIC Radio Occultation observations during the ascending phase of solar cycle 24. *Adv. Space Res*., **60**, 2017.

Shunk, R. and Nagy, A. Ionospheres: Physics, Plasma Physics, and Chemistry 2nd ed. *Cambridge University Press*, 2009.

Scherliess, L. and Fejer, B. Seasonal and longitudinal variability of low-latitude total electron content tidal influences. *J. Geo phys. Res*., **113**, 2008.

Sojka, J. and Schunk, R. A theoretical study of the global F-region for June solstice, solar maximum and low magnetic activity. *J. Geo phys Res*., **90**, 1985.

Tamirat, B. A study of the equatorial ionization anomaly in Addis Ababa Ethiopia from CHAMP satellite ion density data. 2008.

Yadav, S., Dabas, R., Rupesh, M., and Gwal, A. Temporal and spatial variation of equatorial

ionization anomaly by using multistation ionosonde data for the 19th solar cycle over the Indian region. *Adv. Space Res*., **51**, 2012.

Zhao, B., Liu, L. Wan, W. and Ren, Z. Characteristics of ionospheric total electron content of the equatorial ionization anomaly in the Asian-Australian region during 1996-2004. *Ann. Geo phys*., **27**, 2009.

Zhao, B., Liu, L., Liu, J. Time delay and duration of ionospheric total electron content responses to geomagnetic disturbances. *Beijing China*, 2010.